Design and Evaluation of a Bone Regeneration Conducting Membrane Based on PLCL/Gelatin Containing nHA and β-TCP for Reconstruction of Mandibular Bone Defects

***Tahereh Sadat Tabatabai*[1] *,Taybeh Sadat Tabatabaie*[1*]**

1- Student Research Committee, School of Medicine, Shahroud University of Medical

**: Corresponding author, Dr. Tayebeh Sadat Tabatabai. Email: Tybeh.sadat.tabatabaie1400@gmail.com. Tel: +989104686909, ORCID: 0000-0003-2077-3900*

Abstract

Reconstruction of jaw bone defects is one of the major challenges in tissue engineering and oral and maxillofacial surgery. The aim of this study was to design and fabricate a bone regeneration conducting membrane (GBR) based on poly(L-lactide-co-caprolactone)/gelatin (PLCL/Gelatin) and to investigate the effect of adding hydroxyapatite (nHA) and β-tricalcium phosphate (β-TCP) nanoparticles on the physical, biological, and osteogenic properties of this membrane. In this study, two groups were investigated, including sample 1 (PLCL/Gelatin) as the base group and sample 2 (PLCL/Gelatin/nHA/β-TCP) as the group containing bioactive ceramic compounds. The membranes were prepared using electrospinning and their morphological characteristics were evaluated using scanning electron microscopy (SEM). The results of SEM images showed the formation of a structure consisting of relatively uniform nanofibers and no significant spine structures. Also, the biocompatibility of the samples was evaluated using hemolysis and cytotoxicity tests. Both groups showed favorable biocompatibility and their hemolysis rate was less than 2%. Comparison of the results of the biological tests showed that the addition of nHA and β-TCP to the PLCL/Gelatin scaffold improved the biological performance of the membrane. In the PLCL/Gelatin/nHA/β-TCP group, an increase in formation of mineral deposits were observed compared to the PLCL/Gelatin group, indicating an increased osteogenic potential of this group. Also, the physical properties of the membranes showed that the presence of ceramic compounds affects the water absorption rate and membrane degradation behavior and can provide more suitable conditions for membrane performance in the biological environment. Histological studies using hematoxylin-eosin and Masson's trichrome staining also showed new bone formation and increased collagen deposition in the group containing nHA/β-TCP. Overall, the findings of this study showed that the PLCL/Gelatin/nHA/β-TCP membrane has a more favorable biological and osteogenic potential compared to the PLCL/Gelatin base membrane and can be considered as a promising option for use in the reconstruction of jaw bone defects.

Keywords: *Guided bone regeneration, PLCL, Gelatin, Nanohydroxyapatite, β-tricalcium phosphate, Bone tissue engineering, Jaw bone regeneration.*

1. Introduction

As a metabolically active tissue, bone has a remarkable capacity for regeneration and renewal, and this property plays an important role in maintaining homeostasis of the skeletal system. In addition to providing structural support for the soft tissues of the body, this tissue is considered one of the most important sites of hematopoiesis in adults. Bone also has an inherent capacity for repair and regeneration in response to injury [1]. However, this natural capacity is not sufficient for complete repair in the face of large and complex bone defects, especially in the craniofacial region, and the treatment of such defects remains one of the major clinical challenges in dentistry and oral, maxillofacial surgery [2]. Acquired defects of the craniofacial region can be caused by various factors, including infectious diseases, trauma, skeletal disorders with progressive deformity, tissue removal surgeries following cancer treatment, congenital anomalies, and other pathological conditions. These defects can have significant adverse effects on chewing function, facial aesthetics, and psychological status of patients [3].

One of the common methods for treating defects and reconstructing maxillofacial bones is the use of autologous and allogeneic bone grafts [4]. Despite the advantages of these methods, each has limitations. Autologous bone grafts can be associated with limited access to suitable tissue and donor site complications, while allogeneic grafts may be associated with immune reactions, limited access, and delayed healing. Therefore,

the development of novel biomaterials and therapeutic strategies that can effectively stimulate bone regeneration while reducing treatment complications has received increasing attention [5].

Guided bone regeneration (GBR) has been proposed as one of the recognized strategies for treating bone defects. In this method, the use of a protective barrier membrane prevents the entry of surrounding cells and soft tissues into the defect site and provides sufficient opportunity for the migration, proliferation, and function of osteogenic cells by creating and maintaining a suitable space. This feature is particularly important in the reconstruction of bone defects in the maxillofacial region [6]. However, some conventional GBR membranes have limitations in terms of biological activity and their degradation products may have adverse effects on the tissue environment. These factors can reduce the regeneration performance of the membrane and prevent the achievement of optimal bone repair [7]. Therefore, the design of biodegradable membranes with suitable physical, mechanical, and biological properties is an important research area in the field of bone regeneration. In recent years, biodegradable polymers such as poly(L-lactide-co-caprolactone) (PLCL) and gelatin have been widely investigated in tissue engineering. PLCL is a biocompatible and biodegradable copolymer that has great potential for use in tissue engineering and regenerative medicine applications due to its favorable mechanical properties and tunability of physical properties [8, 9]. Combining PLCL with gelatin can provide the opportunity to simultaneously utilize the desirable properties of a synthetic polymer and a natural protein. Gelatin, as a natural protein derived from collagen, has favorable biocompatibility and the ability to interact well with cells, and therefore has been considered in the design of tissue engineering scaffolds and membranes [10]. However, in order to increase the biological activity and osteogenic potential of these polymer systems, the use of bioactive ceramic compounds such as hydroxyapatite (HA) and β-tricalcium phosphate (β-TCP) has been considered.

Hydroxyapatite is one of the most important ceramic materials used in bone tissue regeneration due to its similarity in mineral composition to the mineral part of natural bone, biocompatibility and suitable bioactivity. Also, β-TCP can provide suitable conditions for the formation and mineralization of bone tissue due to its biodegradability and ability to release calcium and phosphate ions [11, 12]. Combining these ceramic materials with polymer scaffolds can improve the biological and osteogenic properties of the membrane and provide a more suitable environment for the adhesion, proliferation and differentiation of osteogenic cells. From this perspective, the addition of hydroxyapatite nanoparticles (nHA) and β-TCP to the PLCL/Gelatin system can be a suitable strategy to increase the biological performance of the GBR membrane. Considering the importance of the surface and structural properties of the membrane in the bone regeneration process, the manufacturing method also plays an important role in its final performance. Electrospinning is an effective method for producing nanofibrous structures that can create membranes with high specific surface area, suitable porosity, and a structure similar to some properties of the extracellular matrix. Such a structure can improve the interaction between the cell and the scaffold and provide suitable conditions for cellular processes related to bone regeneration. Despite significant advances in the design of biomaterials, there is still a need to develop GBR membranes with an appropriate combination of biocompatibility, desirable structural properties, and osteogenic potential. Therefore, in the present study, a PLCL/Gelatin-based composite membrane was designed and prepared by adding nHA and β-TCP. In this study, the performance of sample 1 (PLCL/Gelatin) as a base membrane was compared with sample 2 (PLCL/Gelatin/nHA/β-TCP) to investigate the effect of the presence of bioactive ceramic compounds on the physical and biological properties of the membrane, including biocompatibility, degradation behavior, water absorption, and osteogenic potential. It is expected that the addition of nHA and β-TCP to the PLCL/Gelatin matrix will improve the membrane performance in the bone regeneration process by creating a more bioactive environment.

2. Materials and Methods

2.1. Materials

All chemicals and reagents used in this study were obtained from reputable domestic and international companies, including Merck (Germany) and Sigma-Aldrich (USA). All materials were used without additional purification and in accordance with the instructions provided by the manufacturer.

2.2. Preparation of PLCL/gelatin membrane

In order to prepare the PLCL/gelatin base membrane, polycaprolactone (PCL) and polylactic acid (PLA) were first dissolved in a chloroform/methanol solvent mixture with a volume ratio of 75:25. The concentrations of PCL and PLA were considered to be 17 and 1 wt%, respectively. Simultaneously, gelatin was dissolved in glacial acetic acid with a concentration of 13 wt/vol%. All solutions were stirred for 24 hours at room temperature using a magnetic stirrer to obtain uniform and homogeneous solutions. After preparing the

polymer solutions, the solutions were loaded into 5 mL syringes and the electrospinning process was performed using an 18-gauge needle. The parameters of the electrospinning process included an applied voltage of 15 kV, an injection rate of 2 mL/h, a distance of 15 cm between the needle tip and the collector, and a rotation speed of the collector of 700 rpm. At the end of the process, a PLCL/gelatin nanofibrous membrane with a uniform and porous structure was formed and collected on the collector. The membrane obtained from this step was considered as sample 1 (PLCL/gelatin).

2.3. Preparation of PLCL/gelatinnHA/β-TCP membrane

To prepare the composite sample, the PLCL/gelatin membrane was subjected to the process of adding bioactive ceramic compounds after preparation. In this step, hydroxyapatite (nHA) and beta-tricalcium phosphate (β-TCP) nanoparticles with particle sizes less than 50 nm were used. The concentrations of nHA and β-TCP were considered to be 20 and 40 wt% of the total polymer weight, respectively. Thus, a PLCL/gelatin composite membrane containing nHA and β-TCP was prepared. This membrane was considered as sample 2 /PLCL/gelatin/nHA/ β-TCP. In order to increase the structural stability of the membranes and improve their resistance in aqueous environments, the prepared membranes were subjected to a cross-linking process. For this purpose, the samples were exposed to glutaraldehyde vapor with a concentration of 22% for 24 hours. After the cross-linking process was completed, the membranes were completely dried and used for the next stages of the experiment. In this study, two main groups of membranes were investigated. Sample 1 consisted of PLCL/gelatin membrane, which was considered as the base membrane. Sample 2 consisted of PLCL/gelatin/nHA/β-TCP composite membrane, which was prepared with the aim of investigating the effect of adding bioactive ceramic compounds on the membrane properties. Therefore, a comparison between these two groups was made with the aim of evaluating the effect of the presence of nHA and β-TCP on the structural, physical and biological properties of PLCL/gelatin membrane.

2.4. Characterization of electrospun membranes under laboratory conditions

2.4.1. Study of membrane morphology by scanning electron microscopy (SEM)

A scanning electron microscope (SEM) was used to investigate the surface morphology, uniformity of nanofiber structure, fiber arrangement, presence of structural defects, and fiber diameter of electrospun membranes. Membrane samples were cut into appropriate dimensions and placed on aluminum supports. Then, in order to increase the electrical conductivity of the sample surface and improve the quality of the images, the surface of the samples was coated with a thin layer of gold. SEM imaging was performed at different magnifications. The resulting images were examined in terms of surface morphology, uniformity of fiber distribution, porosity, presence or absence of defects such as bead formation, and also the distribution of nanoparticles in the nanofiber structure. Also, the fiber diameter was measured using ImageJ software. For each sample, at least 50 fibers were randomly selected from different areas of the images and the average fiber diameter was calculated and reported along with the standard deviation.

2.4.2. FTIR Test

Fourier Transform Infrared Spectroscopy (FTIR) was used to identify the functional groups present in the membranes and to investigate the chemical changes in the membrane structure after the combination of polymers and nanoparticles. The measurements were performed using an FTIR instrument (ABB Bomem, Quebec, Canada) in the wavenumber range of 400 to 4000 cm^{-1} and with a resolution of 4 cm^{-1}. The obtained spectra were analyzed to identify the characteristic functional groups related to PLCL, gelatin, hydroxyapatite and β-TCP and also to investigate possible interactions between the membrane components.

2.4.3. Blood Compatibility Test

The blood compatibility of the prepared membranes was evaluated by examining the degree of hemolysis. In this test, 2 ml of fresh human blood containing anticoagulant was diluted with 2.5 ml of normal saline solution. Then, 0.2 ml of the diluted blood was incubated with each membrane sample at 37°C for 60 minutes. After the end of the incubation time, the samples were centrifuged at 1500 rpm for 10 minutes and the supernatant was collected and transferred to a 96-well plate. The optical absorbance of the samples was measured at a wavelength of 545 nm using a microplate reader (Anthos 2020, Biochrom, Berlin, Germany). For positive control, blood diluted in deionized water was used, and for negative control, blood diluted in normal saline was used. The percentage of hemolysis was calculated using the following standard equation:

$$\text{Percentage of hemolysis} = [(Dt - Dnc) / (Dpc - Dnc)] \times 100$$

Where Dt is the absorbance of the sample, Dnc is the absorbance of the negative control, and Dpc is the absorbance of the positive control.

2.4.4. Blood Clotting Index (BCI)

In order to investigate the effect of direct contact of the prepared membranes with blood and to evaluate their coagulation behavior, the Blood Clotting Index (BCI) test was performed. First, the samples were placed in test containers and equilibrated for one hour at 37°C. Then, 100 µL of human blood containing anticoagulant was added to each sample. After 5 minutes of incubation, 20 µL of 0.2 M $CaCl_2$ solution was added to each sample to initiate the coagulation process. After 5 minutes, 25 mL of distilled water was slowly added to each container and the samples were kept at 37°C for another 5 minutes. Subsequently, the optical absorbance of the supernatant solution was measured at a wavelength of 545 nm. A control sample was also prepared by directly adding 100 µL of blood to 25 mL of distilled water without the presence of the membrane. Blood coagulation index was calculated using the standard BCI equation.

2.4.5. Cell viability assessment with MTT assay

To assess the biocompatibility and cytotoxicity of the prepared membranes, MTT assay was performed on 3T3 fibroblast cell line. In this assay, 1×10^3 cells were cultured on each sample in a 96-well plate. Cell viability and proliferation were assessed after 24 and 72 hours using MTT assay. At each time point, the culture medium was replaced with fresh medium containing MTT solution at a concentration of 5 mg/mL and the samples were incubated for 2 hours at 37°C in the dark. Then DMSO was added to each well to dissolve the formed formazan crystals. The optical absorbance of the samples was measured at a wavelength of 570 nm using a microplate reader. The percentage of cell viability was calculated using the standard equation and reported as a percentage.

2.4.6. Anti-inflammatory activity test

In order to evaluate the anti-inflammatory properties of the samples, a protein denaturation test was performed. For this purpose, 0.1 g of each sample was mixed with 2.8 ml of PBS solution with pH 6.8 and 0.2 ml of 1% albumin solution. The resulting mixture was incubated for 15 minutes at 37°C and then heated for 5 minutes at 70°C.

After that, the optical absorption of the samples was measured at a wavelength of 660 nm. Aspirin was used as a reference standard and a mixture of distilled water and 1% albumin as a control.The percentage of protein denaturation inhibition was calculated using the standard equation.

2.4.7. pH assessment

To investigate the changes in the pH of the medium in contact with the prepared membranes, samples of equal weight were placed in PBS solution. The pH of the solution was measured at specified times. Measurements were performed using a pH meter (pH meter 1140; Mettler Toledo, Greifensee, Switzerland). The changes in the pH of the samples over time were evaluated to investigate chemical stability and possible changes due to material degradation.

2.4.8. Measurement of water contact angle

In order to evaluate the hydrophilicity of the prepared membranes, the static water contact angle was determined using a contact angle measuring device (KRÜSS, Hamburg, Germany). For each sample, a water droplet was placed on three different areas of the membrane surface and the angle formed between the water droplet and the membrane surface was measured. The final contact angle value was reported as the average of the measurements taken.

2.4.9. Weight loss test

The weight loss test was performed to evaluate the stability and degradation rate of the prepared membranes under simulated physiological conditions. First, the initial dry weight of each sample was accurately measured and recorded as W_0. Then, the samples were placed in 10 ml of normal saline and kept in an incubator at 37°C. At the specified times, including 2, 4, 6 and 12 hours, the samples were taken out and after preparation and drying, their final weight (Wt) was measured. The percentage of weight loss was calculated using the following equation:

$$\text{Weight loss } (\%) = [(W_0 - Wt) / W_0] \times 100$$

2.4.10. Water absorption test

In order to evaluate the water absorption capacity of the membranes, the dried and lyophilized samples were first weighed and their initial weight (M_0) was recorded. Then, the samples were completely immersed in a container containing PBS with a pH of 7.4. The water absorption process was carried out at 30°C for 2 and 4 hours. After each specified time, the samples were quickly removed from the solution, excess water was removed from their surface, and immediately weighed. The weight of the sample in the swollen state was recorded as M_1. The percentage of water absorption or equilibrium swelling was calculated using the following equation:

$$\text{Water absorption (\%)} = [(M_1 - M_0) / M_0] \times 100$$

2.4.11. Alizarin Red S Staining

Extracellular matrix mineralization was assessed using qualitative and quantitative Alizarin Red S staining on days 3, 7, 10, and 21. Following fixation, cell-seeded scaffolds were stained with Alizarin Red S solution to visualize calcium-rich mineralized nodules. For quantitative analysis, the bound dye was extracted and quantified spectrophotometrically. All measurements were performed in sextuplicate (n = 6).

3. Animal Surgery Protocol

All animal procedures were performed after receiving approval from the Ethics Committee of Shahrood University of Medical Sciences (Ethics Code: IR.SHMU.AEC.1403.036). Before surgery, animals were anesthetized with intraperitoneal injection of ketamine at a dose of 100 mg/kg and xylazine at a dose of 10 mg/kg. After ensuring proper anesthesia, the surgical area was shaved and disinfected under aseptic conditions. A bilateral linear incision of 1.5 cm in length was made from the ramus of the mandible to the lower edge of the mandibular body. Then, the soft tissues were gently pushed aside to expose the buccal and lingual cortical surfaces of the mandible. A critical bone defect of 5 mm in diameter and 2 mm in depth was created in the mandibular body, adjacent to the alveolar bone and between the incisors and first molars. Defect creation was performed using a low-speed trephine bur (1000 rpm) and under continuous irrigation with cold sterile saline to prevent thermal injury. In this study, animals were divided into two experimental groups based on the research design:

Group 1 (Sample 1): Bone defect treated with PLCL/Gelatin membrane.

Group 2 (Sample 2): Bone defect treated with PLCL/Gelatin/nHA/β-TCP membrane.

After placing the membrane in the defect site, the muscle layer was sutured with 3-0 absorbable suture and the skin with 3-0 nylon suture. Animals were maintained under standard laboratory conditions after surgery. At designated times after surgery, animals were euthanized and mandibular specimens containing the defect area were collected for radiographic, histological, and histomorphometric examinations. Important note: In the previous text, the surgical evaluation times were mentioned as "2 and 4 months," but in the histology section it was written as "3 months." This must be consistent with the actual time of your test, and both times should not remain in the article.

3.1. Histological evaluation

Hematoxylin-eosin (H&E) and Masson's trichrome staining were used to examine the regenerated tissue. H&E staining was performed to evaluate the general morphology of the regenerated tissue, the extent of inflammatory cell infiltration, new bone formation, and tissue organization in the defect area. Masson's trichrome staining was also used to evaluate the extent of collagen deposition, extracellular matrix formation, and the maturity of the newly formed bone. At the designated time after surgery, the animals were euthanized and mandibular specimens containing the defect area were harvested. The specimens were fixed in 10% neutral buffered formalin for 48 hours. After fixation, the specimens were decalcified, dehydrated, and embedded in paraffin after going through standard procedures. Sections were prepared at 5 µm thickness and then stained with H&E and Masson's trichrome. The specimens were examined using a light microscope (BX51, Olympus, Tokyo, Japan) equipped with a digital camera (DP72, Olympus). Images were recorded at 40×, 100×, and 400× magnifications. Histomorphological parameters including inflammatory response, collagen deposition

rate, new bone formation, bone maturation, and tissue integrity in the defect area were assessed by an independent and blinded evaluator.

3.2. Animal Ethical Considerations

All animal experiments in this study were conducted in accordance with ethical guidelines for the use of laboratory animals. The study protocol was reviewed and approved by the Ethics Committee of Shahrood University of Medical Sciences. In addition, the principles of minimizing animal pain and suffering, using the minimum number of animals required, and observing appropriate housing conditions were considered throughout the study.

4. Statistical Analysis

Statistical analysis of the obtained data was performed using SPSS version 26.0 software. Graphs were prepared using GraphPad Prism version 8.0 software. Regarding the comparison of experimental groups, the differences between the groups were examined using appropriate statistical tests. In cases where more than two groups or more than one time were compared, one-way analysis of variance (One-way ANOVA) and LSD post hoc test were used. Data values were reported as mean ± standard deviation (Mean ± SD) and P value < 0.05 was considered as the level of statistical significance.

5. Results

5.1. Morphology of electrospun membranes

Scanning electron microscope (SEM) images of electrospun membranes in the two studied groups showed (Fig.1.A) that both membranes had a uniform, continuous, and porous nanofibrous structure. In group S1 (PLCL/Gelatin), the fibers were randomly arranged next to each other and formed an interconnected network. No significant breakage, polymer droplets, or bead formation were observed in the images, indicating that the electrospinning process conditions were suitable for the formation of uniform fibers. In group S2 (PLCL/Gelatin/nHA/β-TCP), the overall nanofibrous structure was also maintained. The presence of nHA and β-TCP nanoparticles caused a relative change in the surface morphology of the fibers and increased the surface roughness, however, no severe particle aggregation or significant discontinuity in the fiber structure was observed. Therefore, the addition of mineral phase nHA and β-TCP caused a major disruption in the formation of the non-nanofibrous network and the structural integrity of the membrane was maintained. In general, both groups had porous nanofibrous structures and no major morphological defects, although group S2 showed a relatively rougher surface compared to S1.

5.2. . FTIR spectroscopy study

The FTIR results (fig. 1.B) confirmed the presence of the main components of the membrane in both groups. In the spectrum of group S1, the band corresponding to the carbonyl group C=O of PLCL polymers was observed in the range of 1720–1750 cm^{-1}. Also, the bands in the range of 3200–3500 cm^{-1} were attributed to the stretching vibrations of the O–H and N–H groups present in gelatin. The amide bands in the range of about 1650 cm^{-1} and 1540 cm^{-1} also confirmed the presence of gelatin. In group S2, in addition to the bands related to PLCL and gelatin, an increase in the intensity of the bands related to phosphate groups in the range of 560–600 cm^{-1} and 960–1100 cm^{-1} was observed, which is consistent with the presence of nHA and β-TCP in the membrane structure. Overall, the FTIR results confirmed the successful presence of polymer, gelatin, and the inorganic phase in groups S1 and S2.

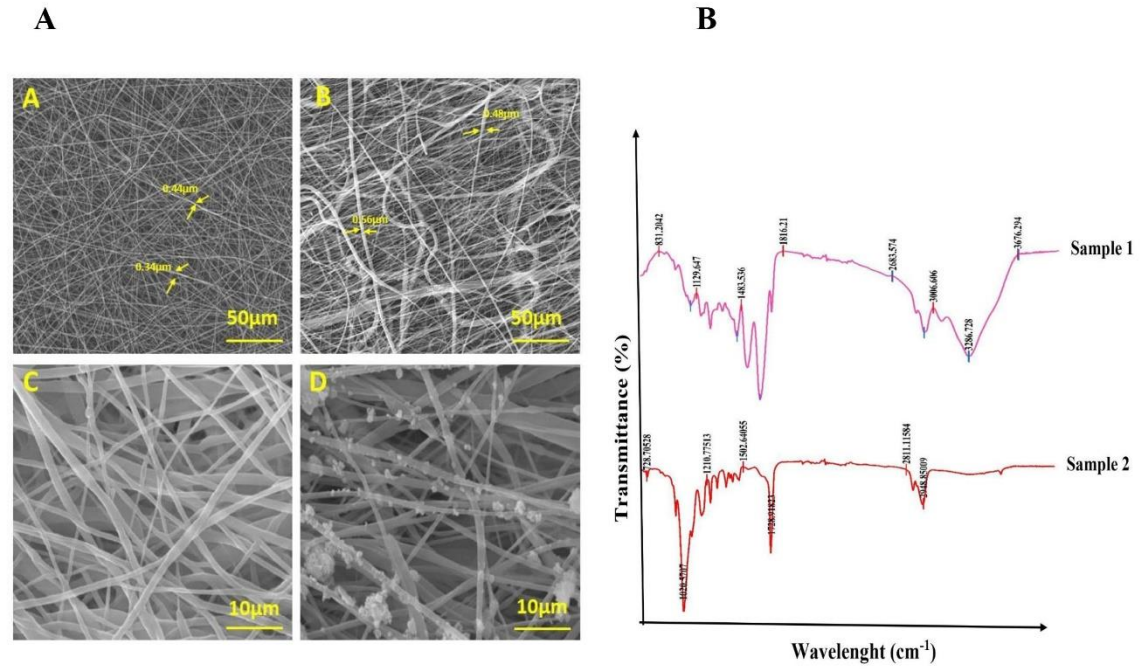


Figure 1. *Morphological and chemical characterization of the electrospun membranes. (A) SEM images of S1 (PLCL/Gelatin) and S2 (PLCL/Gelatin/nHA/β-TCP) membranes, showing uniform and interconnected nanofibrous structures with increased surface roughness in S2. (B) FTIR spectra of S1 and S2 membranes, confirming the characteristic functional groups of PLCL and gelatin, as well as the presence of phosphate groups associated with nHA and β-TCP in S2.*

5.3. Evaluation of hemocompatibility of membranes

The hemocompatibility study (Fig. 2.A) showed that both groups S1 and S2 had a hemolysis percentage of less than 2%. Group S1 showed a hemolysis value of 1.33 ± 0.93%. In group S2, the hemolysis percentage was also in the range of less than 2%. Therefore, both membranes showed favorable behavior in terms of damage to red blood cells, and the addition of nHA and β-TCP did not cause significant hemolysis.

5.4. Evaluation of blood coagulation index

The results of the blood coagulation index test (Fig. 2.B) showed that the composition of the membrane affects its coagulation behavior. Among the two groups studied, group S2 (PLCL/Gelatin/nHA/β-TCP) had a blood coagulation index of 62.10 ± 0.63. Compared to group S1, the difference in coagulation index indicates the effect of the presence of inorganic nanoparticles on the interaction of the membrane surface with blood components.

5.6. Evaluation of cellular biocompatibility with MTT test

The results of the MTT test (Fig. 2.C) showed that in the first 24 hours, both membrane groups had a significant decrease in cell viability compared to the control group ($P<0.05$). With increasing the culture time to 72 hours, a trend of increasing cell viability and proliferation was observed in the groups.

In the comparison between the two groups, the S2 group showed a more favorable cell performance than the S1 group. This increase could be related to the presence of nHA and β-TCP and the provision of more suitable surface conditions for cell adhesion and activity.

5.7. Evaluation of protein degradation inhibition

The results of the protein degradation inhibition test (Fig. 2.D) showed that both groups S1 and S2 had a significant decrease in the percentage of protein degradation inhibition compared to the control group ($P<0.05$). However, the difference between the two groups indicated that the membrane composition could

affect the response related to the inhibition of protein degradation. The presence of nHA and β-TCP in the S2 group caused a difference in this property compared to the basic membrane.

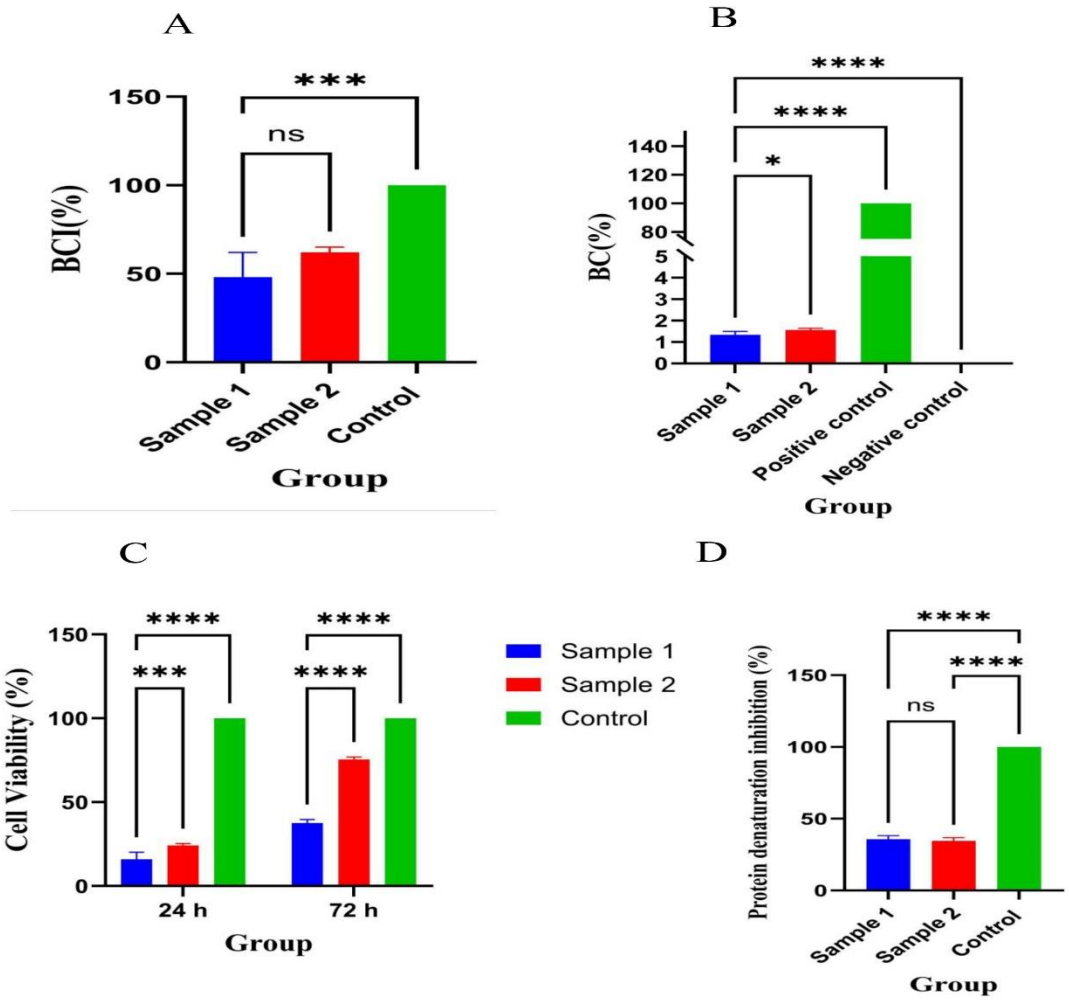


Figure 2. *Evaluation of the biological properties of the electrospun membranes. (A) Hemolysis percentage of S1 (PLCL/Gelatin) and S2 (PLCL/Gelatin/nHA/β-TCP) membranes, demonstrating favorable hemocompatibility with hemolysis values below 2%. (B) Blood coagulation index of the membranes, showing the effect of membrane composition on blood coagulation behavior. (C) Cell viability and proliferation assessed by the MTT assay after 24 and 72 h of culture. (D) Protein degradation inhibition of S1 and S2 membranes compared with the control group. Data are presented as mean ± SD.*

5.8. Investigation of changes in the pH of the environment

Investigation of the pH of the environment during the study period (Fig.3.A) showed that both groups S1 and S2 were able to maintain the pH in an almost neutral range, around 7. No significant change in the pH of the medium was observed, and the presence of nHA and β-TCP in group S2 did not cause any adverse changes in the environmental conditions. The relative stability of the pH indicates the appropriate chemical behavior of the membranes in the studied environment.

5.9. Investigation of the hydrophilicity of the membrane surface

The results of the water contact angle test (Fig.3.B) showed that group S2 had a lower contact angle than group S1. Therefore, the addition of nHA and β-TCP increased the hydrophilicity of the membrane surface.

The decrease in the water contact angle in group S2 indicates that the presence of the mineral phase improved the interaction of the membrane surface with water. This feature can be related to increased water absorption and improved surface conditions for the interaction of cells with the membrane.

5.10. Evaluation of water absorption of membranes

The results of the water absorption test (Fig.3.C) showed that both groups showed an increase in water absorption with increasing time. Group S1 showed the lowest water absorption compared to group S2, while the presence of nHA and β-TCP in group S2 was associated with an increase in water absorption capacity. The increase in water absorption in group S2 can be attributed to the change in the surface properties of the membrane due to the presence of the mineral phase. Also, the presence of gelatin in the structure of both groups caused the creation of hydrophilic functional groups and increased the ability of the membrane to interact with the aqueous environment. In general, group S2 showed a higher capacity for water absorption compared to the base group S1.

5.11. Evaluation of the weight loss of membranes

The results of the weight loss test (Fig.3.D) showed that both membranes experienced a gradual weight loss with increasing incubation time, which indicates the gradual destruction of the structure in the studied environment. Group S1 showed the lowest weight loss, while group S2 had a greater weight loss. The increase in the degradation rate in group S2 could be related to the presence of nHA and β-TCP and the change in the surface properties and interaction of the membrane with the aqueous environment. Therefore, the addition of the mineral phase to the PLCL/Gelatin structure caused a change in the degradation behavior of the membrane.

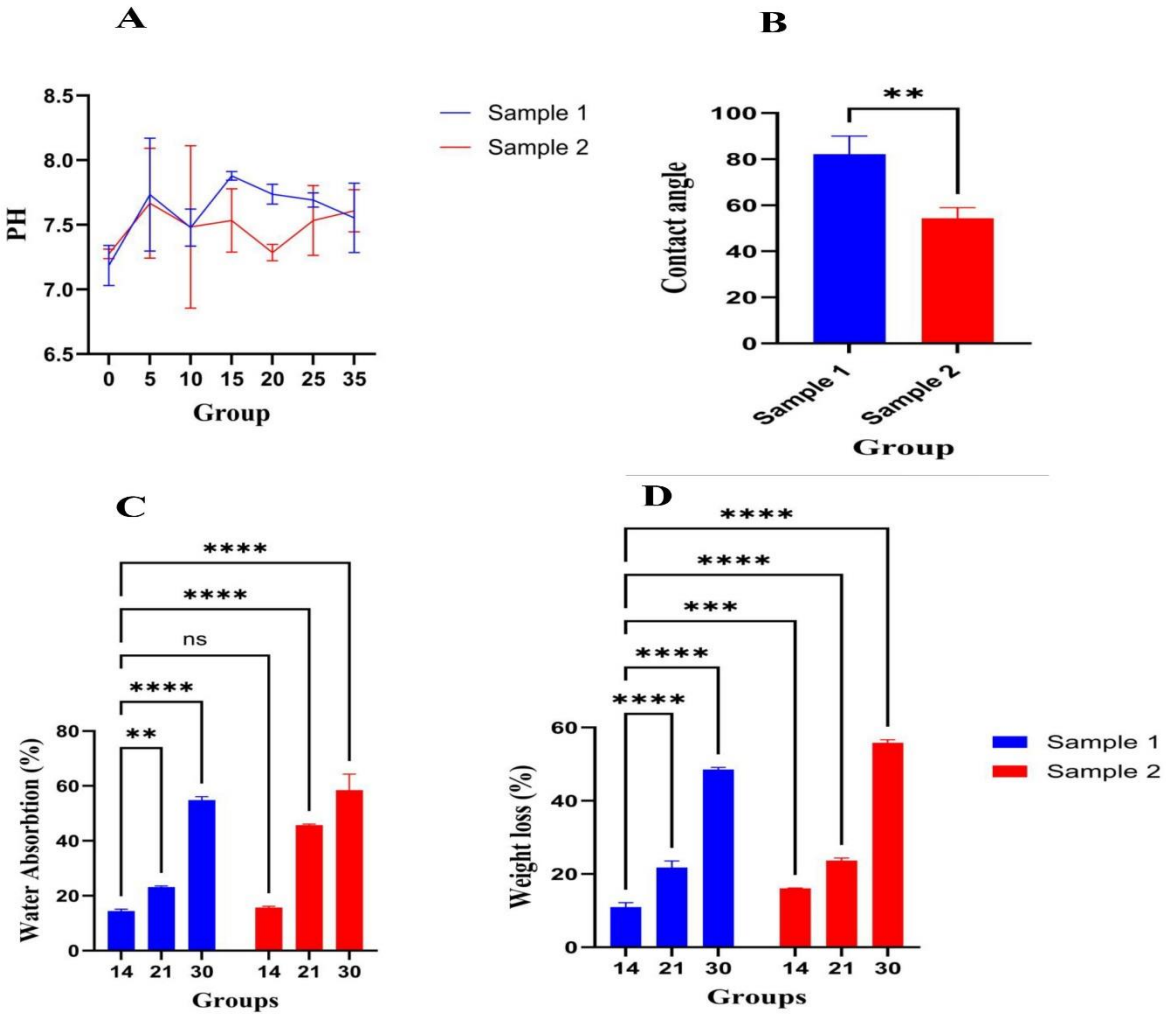


Figure 3. *Evaluation of the physicochemical properties of the electrospun membranes. (A) Changes in the pH of the culture medium during the study period for S1 (PLCL/Gelatin) and S2 (PLCL/Gelatin/nHA/β-TCP) membranes. (B) Water contact angle measurements showing the effect of nHA and β-TCP incorporation on the surface hydrophilicity of the membranes. (C) Water absorption capacity of S1 and S2 membranes at different time points. (D) Weight loss of the membranes during incubation, indicating their degradation behavior over time. Data are presented as mean ± SD.*

5.12. Evaluation of mineral deposit formation by Alizarin Red staining

The results of Alizarin Red staining showed that the amount of calcium deposit formation increased with increasing culture time (3,7,10 and 21 day).(Fig4,5) In the early stages of culture, the difference between groups was limited, but with increasing time, the formation of mineral deposits in the groups increased. Group S2 showed a higher staining intensity compared to S1, indicating an increase in the formation of calcium deposits and mineralization of the extracellular matrix in the presence of nHA and β-TCP. This finding indicates that the presence of a mineral phase in the S2 membrane can provide more suitable conditions for the mineralization process and osteogenic response of cells.

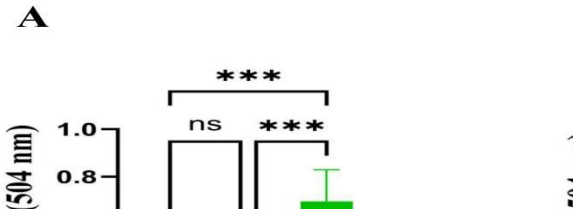


Figure 4. *Evaluation of calcium mineral deposition in S1 (PLCL/Gelatin) and S2 (PLCL/Gelatin/nHA/β-TCP) membranes by Alizarin Red staining. (A) Day 3, (B) Day 7, (C) Day 10, and (D) Day 21 of culture. The intensity of Alizarin Red staining increased with increasing culture time, with S2 showing greater calcium deposition and mineralization compared with S1.*

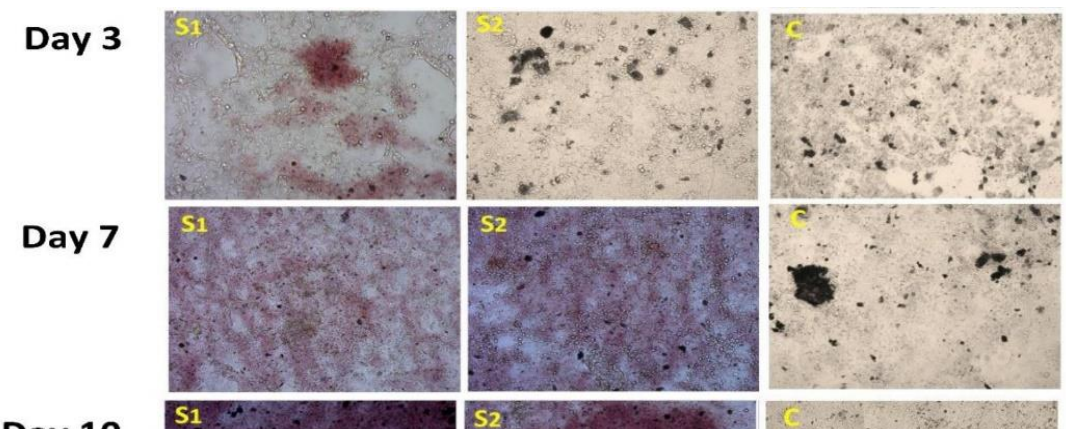


Figure 5. *Evaluation of calcium mineral deposition in S1 (PLCL/Gelatin) and S2 (PLCL/Gelatin/nHA/β-TCP) membranes by Alizarin Red staining. At day 3, day 7, day 10, and day 21 of culture. The intensity of Alizarin Red staining increased with increasing culture time, with S2 showing greater calcium deposition and mineralization compared with S1.*

5.13. Histological evaluation with hematoxylin-eosin (H&E) staining

The results of hematoxylin-eosin (H&E) staining after 3 months of jaw bone defect creation showed (Fig.5) differences in the rate of bone tissue regeneration between the two study groups. In group S1 (PLCL/Gelatin), the defect area was mainly filled with fibrous connective tissue and the rate of new bone formation was limited. Also, in some areas, empty spaces and complete lack of bone tissue continuity were visible at the defect site. In group S2 (PLCL/Gelatin/nHA/β-TCP), the rate of new bone formation increased compared to group S1. In this group, new bone trabeculae with greater organization were observed in the defect area and there was a relative reduction of fibrous connective tissue along with increased cellular infiltration at the defect site. Also, the presence of areas containing newly formed bone and active osteoblasts indicated a greater progress of the bone regeneration process compared to group S1. Overall, the H&E staining findings showed that the addition of nHA and β-TCP to the PLCL/Gelatin construct improved new bone formation and reduced fibrous tissue at the defect site.

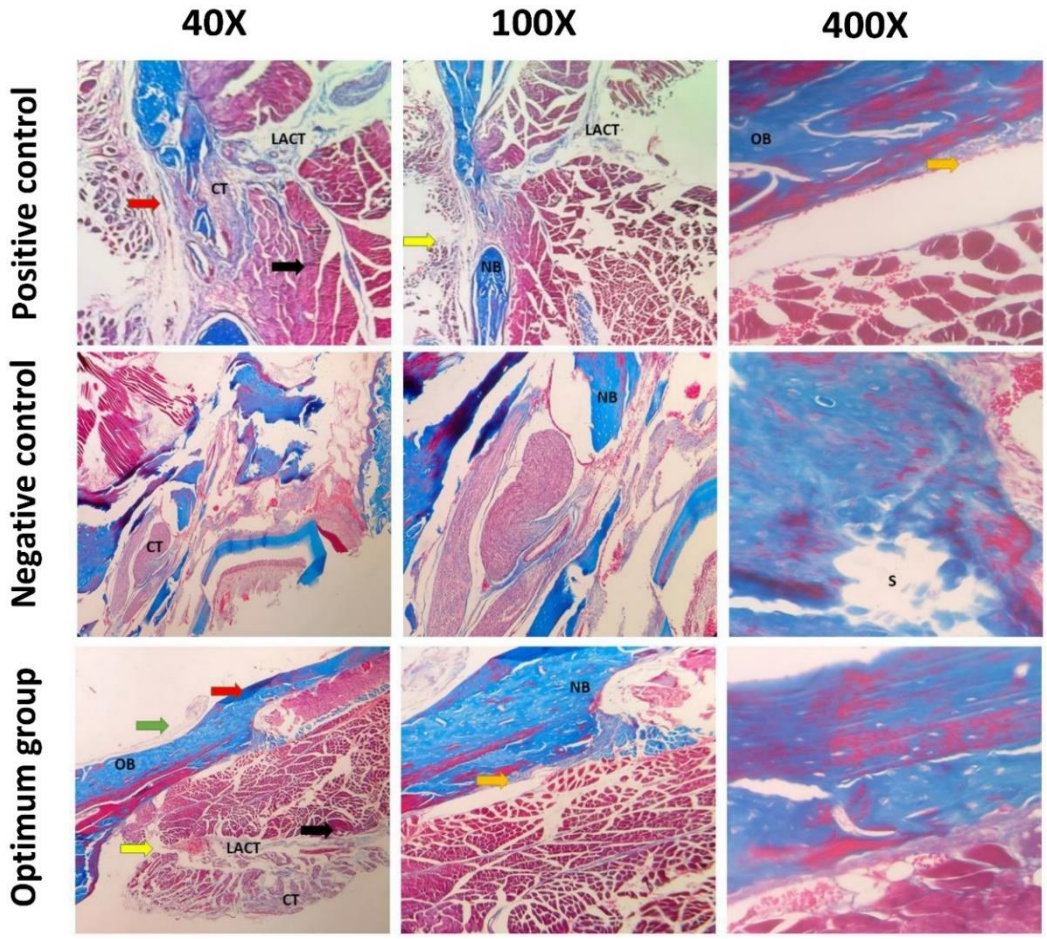


Figure 5: Histological images of hematoxylin-eosin (H&E) staining of the jaw bone defect area after 3 months in the negative control, positive control, and optimal membrane-treated groups (S5). Increased new bone formation and decreased fibrous tissue were observed in the S2 group. LACT, loose areolar connective tissue; OB, old bone; NB, new bone; S, scaffold; CT, connective tissue; Black arrow, newly formed blood vessels; red arrow, bone marrow; blue arrow, osteocyte; yellow arrow, endosteum; green arrow, periosteum; Orange arrow, osteoblast.

5.14. Assessment of collagen matrix formation by Masson's Trichrome staining

The results of Masson's Trichrome staining after 3 months (Fig.6) showed that the degree of collagen matrix formation and organization was different in the two groups. In group S1 (PLCL/Gelatin), the amount of collagen fibril deposition in the defect area was relatively limited and the collagen fibrils were less organized. A significant portion of the defect area was still occupied by immature connective tissue. In contrast, in group S2 (PLCL/Gelatin/nHA/β-TCP), an increase in the amount of collagen fibril deposition and density was observed in the defect area. The collagen fibrils were more organized and had a better relationship with the newly formed bone areas. This finding indicates better formation of extracellular matrix and greater progress of bone tissue regeneration process in group S2 compared to S1. Overall, the results of Masson's trichrome staining showed that the presence of nHA and β-TCP in PLCL/Gelatin membrane was associated with increased formation and organization of collagen matrix and could improve the bone regeneration process compared to the basement membrane. Overall, both histological evaluations showed that S2 (PLCL/Gelatin/nHA/β-TCP) performed better than S1 (PLCL/Gelatin) in bone defect regeneration. Increased new bone formation in H&E and increased collagen deposition and organization in Masson's trichrome staining indicated the positive role of adding nHA and β-TCP in improving the bone tissue regeneration process.

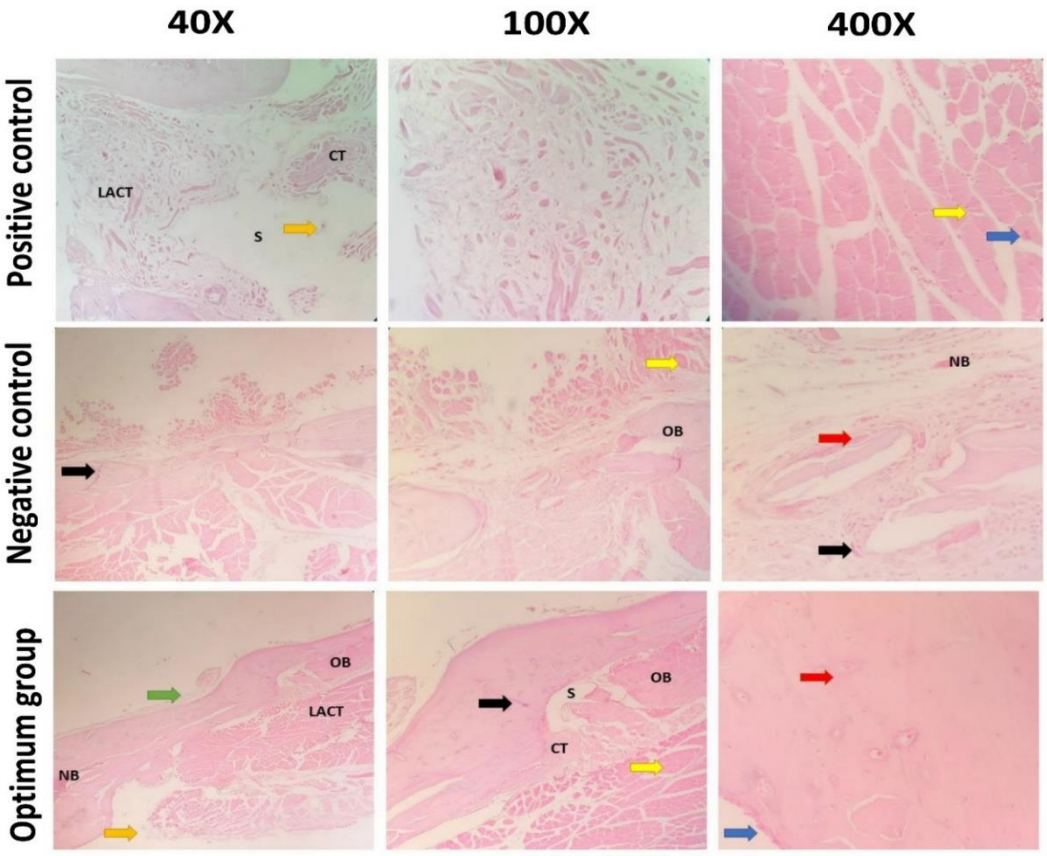


Figure 6: Masson's trichrome staining images of the jaw bone defect area after 3 months. More collagen fiber deposition and organization were observed in the S2 group compared to the control groups. LACT, loose areolar connective tissue; OB, old bone; NB, new bone; S, scaffold; CT, connective tissue; Black arrow, newly formed blood vessels, red arrow, bone marrow; blue arrow, osteocyte; yellow arrow, endosteum; green arrow, periosteum; Orange arrow, osteoblast.

6. Discussion

In the present study, two types of electrospun membranes based on PLCL/Gelatin with and without the addition of nHA and β-TCP nanoparticles were designed and evaluated. The main objective was to investigate the effect of adding bioactive mineral phases on the physicochemical, mechanical, biological and bone regeneration performance of the membranes. The results of the studies showed that the addition of nHA and β-TCP changed the structural and functional properties of the PLCL/Gelatin membrane and, overall, improved its performance in relation to bone tissue engineering applications.

In examining the morphology of the membranes, both groups S1 (PLCL/Gelatin) and S2 (PLCL/Gelatin/nHA/β-TCP) had a uniform, continuous and porous nanofibrous structure, and no significant bead structures were observed on the fiber surface. This finding indicates that the electrospinning process conditions and the concentration of polymers used were suitable for the formation of stable fibers. In group S2, the presence of mineral nanoparticles was associated with a relative increase in surface roughness, while the overall integrity of the fiber network was maintained. Maintaining a continuous and porous structure is important for GBR membranes, because this structure can provide a suitable substrate for cell interaction with the scaffold surface.

The presence of gelatin in the membrane structure can also play a role in creating suitable biological properties. Gelatin, with its hydrophilic functional groups, can improve the surface properties of the membrane and provide more suitable conditions for cell-scaffold interaction. On the other hand, the addition of nHA and β-TCP in group S2 resulted in the introduction of a bioactive mineral phase into the membrane structure, which is more similar in composition to the mineral part of bone tissue.

The FTIR test results also confirmed the presence of the main components of the membrane. The band related to the carbonyl group in the range of 1720–1750 cm^{-1} indicated the presence of the ester structure of PLCL, while the bands related to the O–H and N–H groups as well as the amide bonds confirmed the presence of gelatin. In group S2, the increase in the bands related to the phosphate groups in the range of 560–600 and 960–1100 cm^{-1} also corresponded to the presence of the mineral phases nHA and β-TCP. Therefore, the FTIR results showed that the addition of the mineral phase to the PLCL/Gelatin membrane was accompanied by the preservation of the main structural components.

The results of the water absorption test showed that both groups showed an increase in water absorption with increasing time. However, the S2 group had a higher water absorption rate than S1. This increase can be attributed to the presence of gelatin and mineral nanoparticles and the increased hydrophilic properties of the membrane surface. Proper water absorption is important for tissue engineering scaffolds, as a suitable aqueous environment can facilitate the transport of nutrients and metabolites and provide more suitable conditions for cellular activity.

The results of the water absorption test showed that both groups showed an increase in water absorption with increasing time. However, the S2 group had a higher water absorption rate than S1. This increase can be attributed to the presence of gelatin and mineral nanoparticles and the increased hydrophilic properties of the membrane surface. Proper water absorption is important for tissue engineering scaffolds, as a suitable aqueous environment can facilitate the transport of nutrients and metabolites and provide more suitable conditions for cellular activity.

The results of the weight loss test also showed that the rate of membrane degradation increased over time. Group S1 showed the lowest weight loss, while group S2 showed a greater rate of weight loss during the study period. This difference can be related to the increased water absorption and penetration of the aqueous environment into the membrane structure in the group containing nanoparticles. Increased water penetration into the network can facilitate the degradation processes and structural changes of the membrane.

Despite the difference in the degradation rate, the pH of the environment showed that both groups were able to maintain relatively stable conditions close to the neutral range during the study period. The lack of observation of severe pH changes indicates that the membrane degradation process under the experimental conditions did not lead to undesirable changes in the environment. Maintaining appropriate environmental conditions is important for cell survival and scaffold biological function.

In the hydrophilicity study, group S2 also showed a lower water contact angle than group S1. The decrease in contact angle indicates an increase in the hydrophilicity of the membrane surface. This finding is consistent with the results of the water absorption test and indicates that the presence of nHA and β-TCP can change the surface properties of the membrane towards increased interaction with the aqueous environment. Increased surface hydrophilicity can be effective in creating more suitable conditions for cell adhesion and activity.

The results of the MTT test also showed that the cellular response changed over time and increased at 72 hours compared to 24 hours. This trend indicates the gradual adaptation of cells to the membrane surface and an increase in their metabolic activity over time. Based on the results obtained, group S2 showed a more favorable cellular function than group S1. This improvement can be attributed to more suitable surface properties and the presence of bioactive mineral phases in group S2.

Alizarin Red staining results also confirmed this finding. In the early stages of culture, the difference between the groups was limited, but with increasing culture time, the amount of mineral deposits formed increased. On day 21, group S2 showed a higher amount of mineral deposits formed than group S1. The increased mineralization in group S2 could indicate a higher potential of this membrane to support osteogenic differentiation and mineral matrix formation.

The presence of nHA and β-TCP in group S2 could be one of the main factors for the increased osteogenic activity. These minerals can create more suitable conditions for bone cell activity by providing an environment more similar to the mineral phase of bone. Therefore, the increase in ALP and the formation of more calcium deposits in group S2 indicate that the modification of PLCL/Gelatin membrane with these two mineral phases has increased its capacity for bone regeneration applications.

Histological results also confirmed the findings from in vitro tests. In H&E staining, group S1 showed a more limited amount of new bone formation and a greater amount of fibrous connective tissue in the defect area. In contrast, in group S2, more new bone formation, better organization of bone tissue, and a relative reduction

of fibrous tissue were observed. This finding indicates a better performance of the membrane containing nHA and β-TCP in supporting bone regeneration.
The results of Masson's Trichrome staining also showed that group S2 had a greater amount and better organization of collagen fibers in the defect area. In group S1, more limited collagen deposition and less matrix organization were observed. The increased collagen deposition and organization in group S2 could indicate a more appropriate formation of extracellular matrix and further progress of the bone repair process.
Overall, the comparison of the two groups showed that S2 (PLCL/Gelatin/nHA/β-TCP) performed more favorably than S1 (PLCL/Gelatin) in many of the indicators studied. These advantages included improved mechanical properties, increased hydrophilicity and water absorption, more favorable cellular response, reduced LDH release, increased ALP activity, increased matrix mineralization, and improved bone formation and collagen matrix in histological evaluation. Therefore, the addition of nHA and β-TCP can be considered as an effective strategy to improve the performance of PLCL/Gelatin membrane in bone regeneration applications.

7. Conclusion

In this study, two types of electrospun membranes, including S1 (PLCL/Gelatin) and S2 (PLCL/Gelatin/nHA/β-TCP), were prepared and evaluated for structural, mechanical, and biological properties. SEM results showed that both groups had a network of uniform, continuous, and porous fibers, and no significant bead structures were observed. In group S2, the presence of inorganic nanoparticles caused a relative increase in surface roughness, while the overall nanofibrous structure was maintained. Biologically, MTT results indicated a more favorable cellular response of group S2 compared to S1. Increased mineral deposition in Alizarin Red staining also indicated that the S2 group had higher osteogenic potential. Histological results of H&E and Masson's Trichrome also confirmed the superiority of the S2 group. In this group, more new bone formation, reduced fibrous tissue, and increased deposition and organization of the collagen matrix were observed. Overall, the findings of this study indicate that the addition of nHA and β-TCP to the PLCL/Gelatin membrane simultaneously improved its mechanical, surface, and biological properties, increasing the potential of this membrane for use in guided bone regeneration (GBR).

8. Limitations and Suggestions for Future Studies

Despite the favorable results obtained in the S2 group, the present study has limitations that can be addressed in future research. First, histological evaluation was performed over a three-month period. Examining samples at multiple time points can provide more accurate information about the process of new bone formation, bone tissue maturation, and membrane degradation. Second, to more accurately evaluate bone regeneration, the use of quantitative imaging methods such as Micro-CT can be suggested in future studies. This method allows for the assessment of new bone volume, bone density, and defect filling rate. Also, examining the expression of molecular markers related to bone formation, including Runx2, ALP, Osteocalcin, Osteopontin, and Collagen I, can provide a more detailed understanding of the mechanism of action of nHA and β-TCP on osteogenic differentiation of cells. On the other hand, investigating the mechanical behavior and degradation of the membrane over longer periods of time can provide more information about its structural stability under conditions similar to the physiological environment. Finally, animal studies with larger sample sizes and more suitable animal models can be necessary to confirm the usability of the PLCL/Gelatin/nHA/β-TCP membrane in bone defect reconstruction. Overall, the results of this study show that S2 has a more favorable performance than S1 and the addition of nHA and β-TCP can be an effective approach to improve the performance of the PLCL/Gelatin membrane in GBR applications.

***Reference**:*

1. *Manzini, B.M., et al., Advances in Bone tissue engineering: A fundamental review: BM Manzini et al. Journal of biosciences, 2021.* ***46****(1): p. 17.*
2. *Kämmerer, P.W. and B. Al-Nawas, Bone reconstruction of extensive maxillomandibular defects in adults. Periodontology 2000, 2023.* ***93****(1): p. 340-357.*

3. *Pourlak, T., et al., Usage of stem cells in oral and maxillofacial region. Journal of Stomatology, Oral and Maxillofacial Surgery, 2021.* ***122****(4): p. 441-452.*
4. *Goh, E., N. Beech, and N. Johnson, Traumatic maxillofacial and brain injuries: a systematic review. International journal of oral and maxillofacial surgery, 2021.* ***50****(8): p. 1027-1033.*
5. *Liu, P., et al., Application of dental pulp stem cells in oral maxillofacial tissue engineering. International journal of medical sciences, 2022.* ***19****(2): p. 310.*
6. *Kim, Y.-K. and J.-K. Ku, Guided bone regeneration. Journal of the Korean Association of Oral and Maxillofacial Surgeons, 2020.* ***46****(5): p. 361-366.*
7. *Gedik, B. and M.A. Erdem, The Role and Future of Synthetic Gbr Membranes in Modern Oral and Maxillofacial Surgery. Medical Records, 2026(1).*
8. *Zhao, Y. and H. Liu, Application of PLCL as a biodegradable polymer in biomedical engineering. Journal of Materials Science: Materials in Medicine, 2026.* ***37****(1): p. 46.*
9. *Al-Bishari, A.M., et al., Triple-layered multi-functional membrane for synergistic enhancement of guided bone regeneration. Materials & Design, 2024.* ***239****: p. 112816.*
10. *Zahrin, S.A.b., et al., A review of gelatine: multifunctional additives in the food industry. 2025.*
11. *Mahmoud, A.H., et al., Nanoscale β-TCP-Laden GelMA/PCL Composite Membrane for Guided Bone Regeneration. ACS applied materials & interfaces, 2023.* ***15****(27): p. 32121-32135.*
12. *Akhavan, B.J., N.R. Khanna, and P. Vijhani, Amoxicillin, in StatPearls [Internet]. 2023, StatPearls Publishing.*